

# THE EFFECT OF REPEATED LOADING ON THE GENERATED PRESSURE IN A GIRDLE HIGH PRESSURE APPARATUS

By

Mitsuhiko SHIMADA

(Received August 28, 1974)

## Abstract

The pressure generated by the repeated loading in a girdle high pressure apparatus was calibrated for the purpose of measuring the geophysically important properties at high pressures and temperatures. The calibration was based on the transition in bismuth, thallium, cesium and barium at room temperature, and on the quartz-coesite and coesite-stishovite transitions at high temperatures.

The press load necessary for each calibrated transition decreased with frequency of repetition approaching asymptotically a convergent value. The convergent value was attained by the five time repetition up to 50 kb of sample pressure and by the ten time repetition up to 80 kb. The efficiency of the generated pressure to applied load at 70 kb was 51% in the first loading, 58% in the second and finally attained to 66%. The calibration curves at room temperature were applicable at high temperatures.

## 1. Introduction

In measuring the geophysically important properties like elastic wave velocity, electrical conductivity or thermal diffusivity under high pressures and temperatures, pressure is continuously or stepwise increased and decreased several times a run by means of loading and unloading (e.g. Matsushima [1972], Watanabe [1972], Yukutake [1974]). In the quenching method which is usually used in the investigation of the phase changes of silicates, various procedures of achieving the expected pressure and temperature are used when the experimental conditions are changed from the high pressure phase to the low, or from the liquidus phase to the solidus (e.g. Shimada [1972]).

In the single-stage piston-cylinder apparatus in which the total force on the press ram is applied to the pressure transmitting medium including the sample, the accurate pressure is available in spite of the repeated procedures of load if the magnitude of friction is only measured (Shimada [1971]). However, in the anvil type apparatus like belt, girdle and multi-anvil type, the total force is applied not only to the sample part but to the compressible gasket which plays an important role in the generated pressure, thus the generated pressure is considered to be varied by the repetition of load.

In this work the pressure generated by the repeated loading in the girdle apparatus was calibrated for the purpose of using it in the various geophysical works,

In the high pressure geophysical research, the pressure calibration of the used apparatus and the exact estimate of the error in the measurement of pressure are especially important, because the pressure corresponds directly to the depth of the earth and the experimental results united with pressure are converted into the interpretation or hypotheses on the nature of the earth's interior united with depth.

## 2. Apparatus

The girdle apparatus used was similar to such as previously described by Wilson [1960], Daniels and Jones [1961], and Young *et al.* [1963]. The truncated-cone portion of the tungsten carbide opposing piston has a  $32^\circ$  cone angle and 10 mm piston face in diameter. The tungsten carbide die has a  $32^\circ$  cone angle, 10 mm bore diameter and 4 mm bore height. The internal configuration of gasket and specimen cell in the used apparatus is shown in Fig. 1.

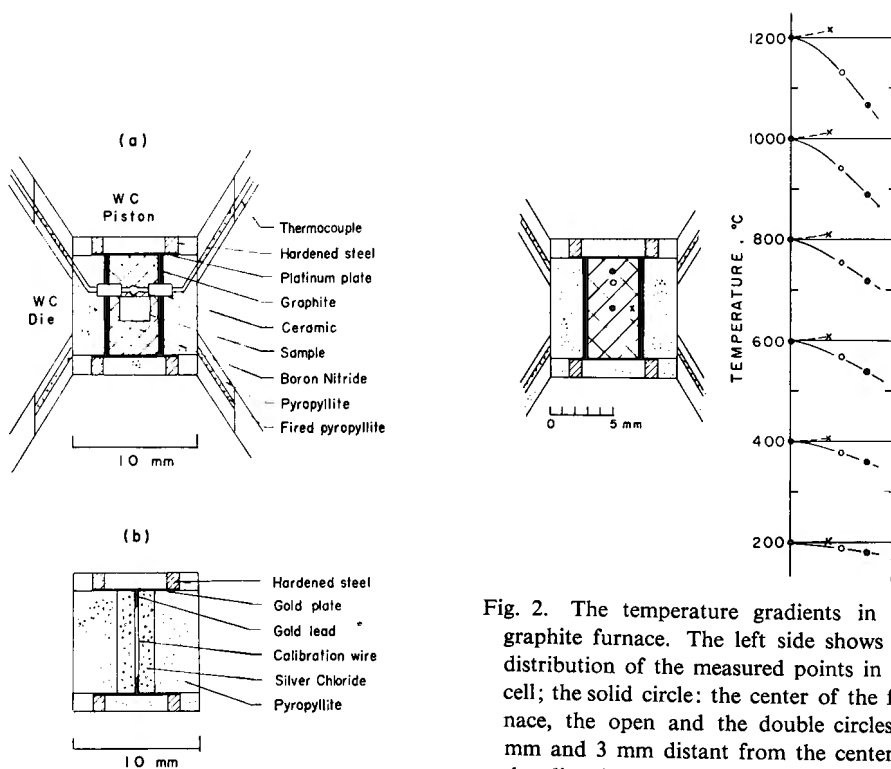


Fig. 1. The internal configuration of gasket and specimen cell. (a) The design used for the quenching method at high temperatures. (b) The cell used for the calibration at room temperature.

Fig. 2. The temperature gradients in the graphite furnace. The left side shows the distribution of the measured points in the cell; the solid circle: the center of the furnace, the open and the double circles: 2 mm and 3 mm distant from the center in the direction of length, respectively, the cross: 1.5 mm distant from the center in the direction of radius. The right side shows the temperatures at the corresponding points as a function of distance from the center.

The dimension of the gasket was determined by the test of the efficiency of the Bi I-II transition pressure to load and by the manageability in assemblage. The cone of fired pyrophyllite was sandwiched in the pyrophyllite gaskets, in which two slots were machined in order to pass the thermocouple wires through them in the high temperature runs. Fig. 2 shows the temperature gradients in the graphite furnace.

### 3. Calibration at room temperature

The calibration was based on the transitions in bismuth of 99.9999% from Osaka Asahi Metal Works, thallium of 99.99% from Mitsuwa Chemical Works, cesium of 99.9% and barium of 99% from Nakarai Chemical Works. The transitions were detected by the changes of the electrical resistance accompanied with the transitions, which are shown in Fig. 3. The pressure scale at 25°C adopted are as follows (Kennedy and LaMori [1962], Lloyd [1971]); Bi I-II:  $25.50 \pm 0.02$  kb, Bi II-III:  $26.96 \pm 0.18$  kb, Tl II-III:  $36.7 \pm 0.3$  kb, Cs II-III:  $42.5 \pm 1.0$  kb, Ba I-II:  $55 \pm 2$  kb, Bi III-V:  $77 \pm 3$  kb. The correction for the difference of the experimental temperature from 25°C was carried out by using the slopes of the phase diagrams determined by Klement *et al.* [1963], Jayaraman *et al.* [1963], Jayaraman *et al.* [1967] and Haygarth *et al.* [1969].

As usually carried out by every worker, the calibration curve for the first loading was obtained from several runs of each transition as shown in Fig. 3. Fig. 4 presents the calibration curve in terms of sample pressure versus press load, in which the efficiencies calculated by the formula: generated pressure/(applied load/cross-sectional area of piston face), is also illustrated by the dashed lines, and Fig. 5 presents in terms of sample pressure versus piston advance. As to the latter, the systematic

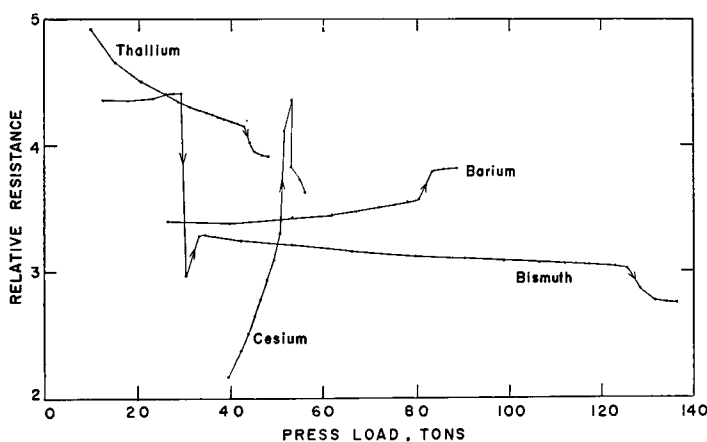


Fig. 3. Typical resistance changes of bismuth, thallium, cesium and barium observed in the cell shown in Fig. 1b.

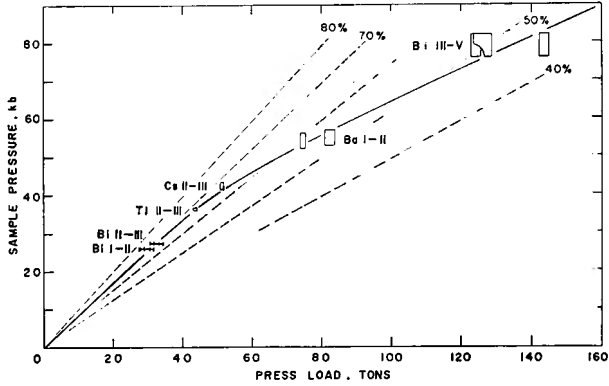


Fig. 4. Pressure calibration curve of the girdle apparatus for the first loading. The dashed lines are the efficiencies of the generated pressure to applied load.

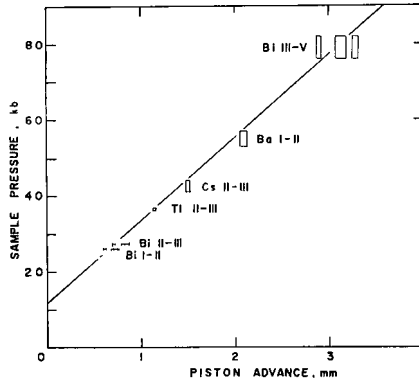


Fig. 5. Relationship between sample pressure and piston advance of the girdle apparatus for the first loading. Piston advance is normalized at the value for 13.43 ton of press load.

relation between sample pressure and piston advance could not be obtained in the repeated loading, but only in the first loading.

The hysteresis phenomenon found in calibration tests on loading and unloading is well known, but the phenomenon in repeating the cycle on loading and unloading has not discussed, of which observation is one of the objects of this work. Fig. 6 shows the typical cycles through the Bi III-V transition with the corresponding ones of piston travel. The load necessary for the transition decreases with frequency of repetition of the cycles on loading and unloading and is likely to be convergent. The typical relations between the frequency of repetition and the load for each transition is shown in Fig. 7. From Fig. 7, it is seen in the case of loading that the load is convergent at the five time repetition up to the pressure of the Cs II-III transition, at the ten time one in the Ba I-II and at the twenty time one in the Bi III-V.

From several runs of each transition, the calibration curves for every frequency

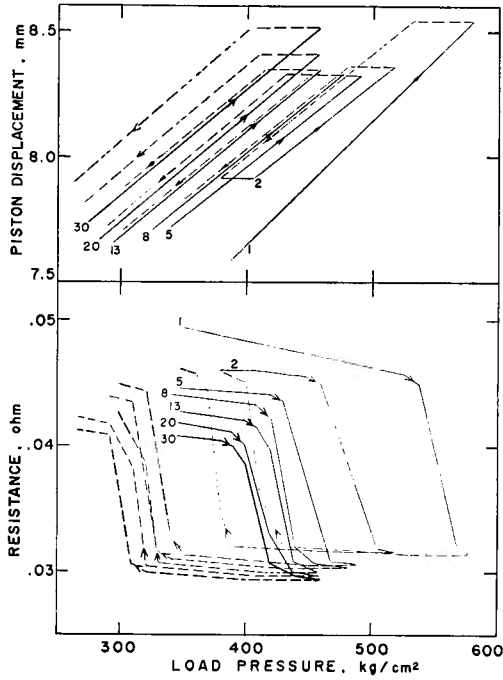


Fig. 6. Typical cycles through the Bi III-V transition (lower) and the corresponding ones of piston travel (upper). The solid lines are on loading and the dashed on unloading. The transition points are illustrated by arrows. The number is the frequency of repetition of the cycles on loading and unloading.

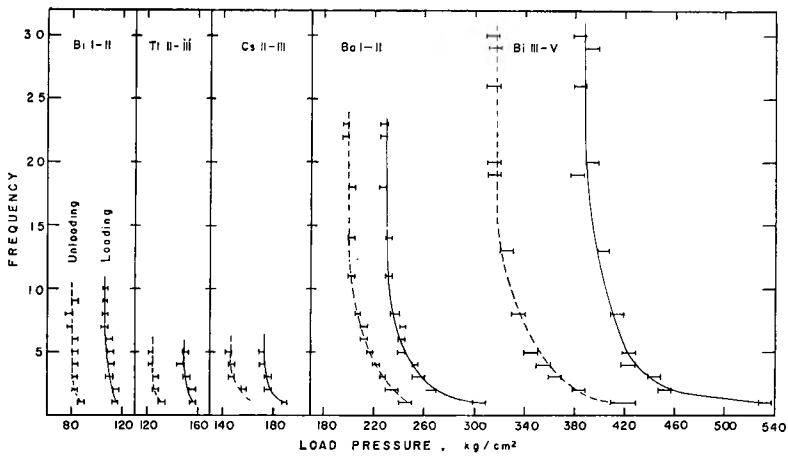


Fig. 7. Typical examples of the effect of repeated loading.

of repetition are obtained and shown in Fig. 8 on loading and unloading. Considering the scattering of runs and the uncertainties caused by the experimental error of each run and by the pressure scale, which are shown in the case of the first loading in Fig. 4, the uncertainty of these calibration curves was estimated at  $\pm 8\%$

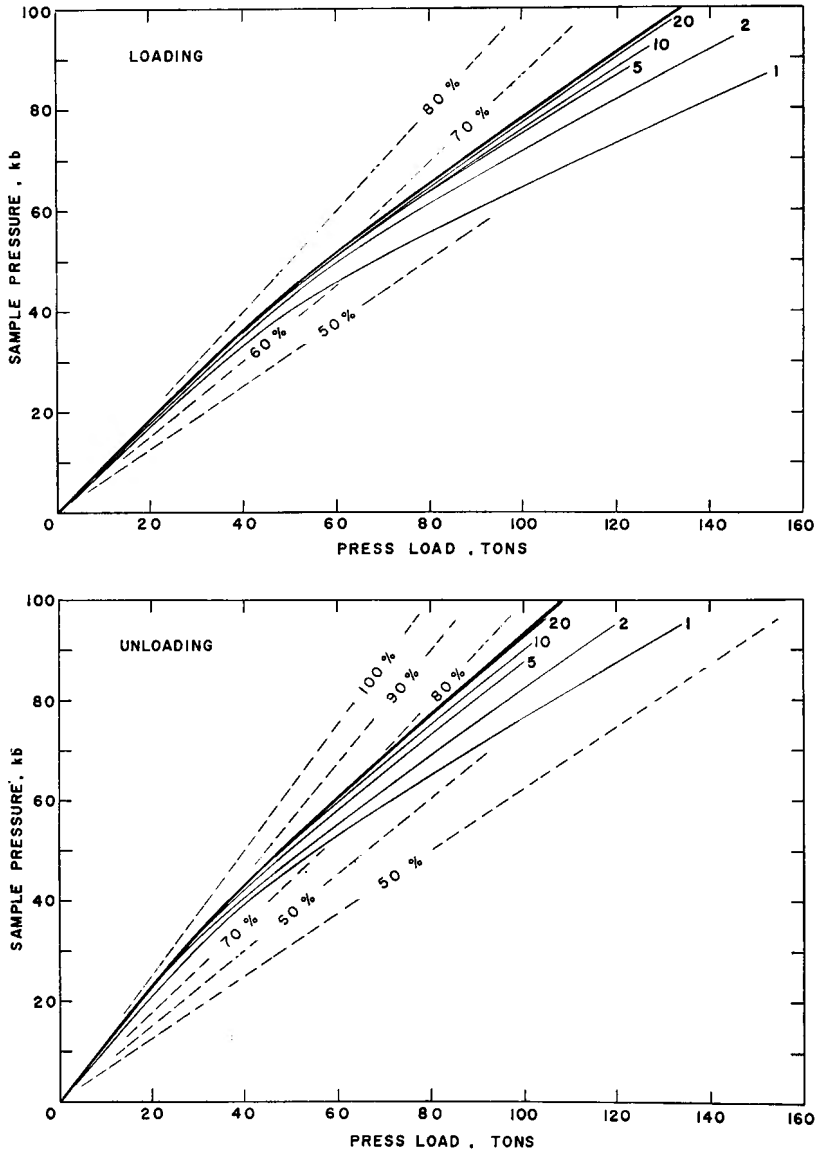


Fig. 8. Pressure calibration curves for every frequency of repetition of the girde apparatus on loading and unloading. The thick curves are from the convergent values. The dashed lines are the efficiencies. The number is the frequency of repetition.

of sample pressure, for instance  $\pm 4$  kb for 50 kb of sample pressure. The difference among the calibration curves of more-than-five time repetition is not meaningful, but the convergent values are considered to be sufficiently attained by the five time repetition.

In the repeated loading or unloading through the whole pressure range illustrated in Fig. 8 except the first loading, the calibration curves are not applicable in the lower pressure range than about 30 kb. In other words, when the load is once lowered below 30 kb after repetition above 30 kb, the calibration curves of the following cycles are far from such as shown in Fig. 8. This is considered to be caused by the break of the linear relationship between load and piston displacement, which is related to the mechanical properties of pyrophyllite used as both the gasket material and the pressure medium. As far as the linear relationship is satisfied, even locally as shown in Fig. 5 (upper), the calibration curves are applicable. The linearity is largely broken below about 30 ton of load in loading runs and below about 25 ton in unloading runs, corresponding to about 30 kb of sample pressure.

It should be noted that in the region where the initial small compression gives rise to the large displacement, if the load is once reduced, the load necessary to generate the same sample pressure is much larger than what otherwise would be.

#### 4. Application at high temperatures

To examine how the effect of repeated loading mentioned above will be at high temperatures and whether the relations at room temperature are applicable, the quartz-coesite and the coesite-stishovite transitions were investigated using the high temperature cell shown in Fig. 1(a). The transition were determined by the quenching method. Silicic acid of Mallinckrodt AR grade, containing 16.0% of water and 0.20% of elements nonvolatile with HF acid, was used as the starting material. A few mg of the sample, without ignition, was sealed in platinum tubing of 1.5 mm in diameter and 0.2 mm in wall thickness. Charges after runs were examined by X-ray diffractometer.

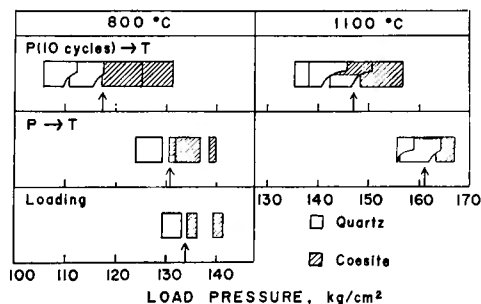


Fig. 9. Results of runs on the quartz-coesite transition. Arrows show the transition points. For other explanation, see text.

The results on the quartz-coesite transition are shown in Fig. 9. Runs of the first loading and the loading after the ten time repetition were carried out at 800°C and 1100°C. To avoid the failure by short circuit caused by the mutual contact of the opposed pistons through the cylinder in repetition of loading and unloading during heating, the loading run was carried out by means of the procedure that the load was raised near the expected one and then temperature was increased. In the first loading at 800°C, runs by this procedure were compared with the real loading runs, or that load was firstly attained to the value corresponding to about 25 kb, then temperature was increased, and finally load was raised to expected one. This comparison is shown in the lower and the middle of the left side in Fig. 9, and is in satisfactory agreement. From this and the experience that on heating at fixed load the piston was displaced to the same direction as loading, it can be allowed to regard the employed procedure as loading one.

The transition points were plotted on the above determined calibration curves at room temperature by adopting the transition pressure of 30 kb at 800°C and 33 kb at 1100°C (Shimada [1974]). These are shown in Fig. 10 in solid circles for the first loading and in open circles for the loading after the ten time repetition.

The coesite-stishovite transition was determined by the same method as the quartz-coesite. Runs of the first loading and the loading after the twenty time repetition were carried out at 600°C. The transition pressure of 84 kb after Akimoto [1972] was adopted. The results are plotted in Fig. 10.

The results at high temperatures are well plotted on the calibration curves at room temperature, considering the uncertainty discussed above. Thus, at high temperatures the sample pressure in the girdle apparatus can be estimated from the

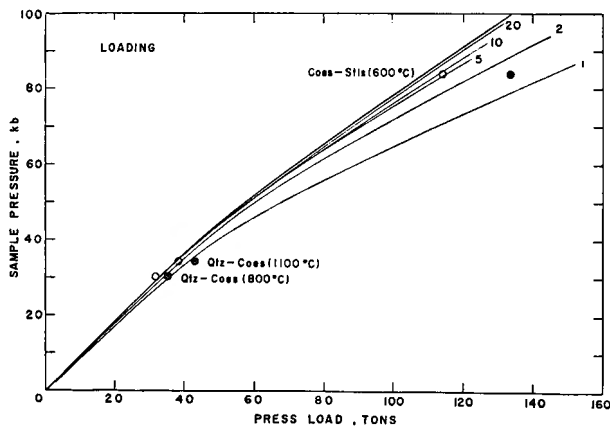


Fig. 10. Comparison of the pressure at high temperatures with the calibration curves at room temperature on loading runs. Solid circles are of the first loading. Open circles are of the loading after the ten time repetition in the quartz-coesite transitions and after the twenty time repetition in the coesite-stishovite transition.

calibration curve at room temperature, at least in the pressure and temperature range examined in this work.

### References

- Akimoto, S., 1972; The system MgO-FeO-SiO<sub>2</sub> at high pressures and temperatures—Phase equilibria and elastic properties, *Tectonophys.*, **13**, 161–187.
- Daniels, W. B. and M. T. Jones, 1961; Simple apparatus for the generation of pressures above 100000 atmospheres simultaneously with temperatures above 3000°C, *Rev. Sci. Instr.*, **32**, 885–888.
- Haygarth, J.C., H.D. Luedmann, I.C. Getting and G.C. Kennedy, 1969; Determination of portions of the bismuth III-V and IV-V equilibrium boundaries in single-stage piston-cylinder apparatus, *J. Phys. Chem. Solids*, **30**, 1417–1424.
- Jayaraman, A., W. Klement, Jr., R.C. Newton and G.C. Kennedy, 1963; Fusion curves and polymorphic transitions of the group III elements—aluminum, gallium, indium and thallium—at high pressures, *J. Phys. Chem. Solids*, **24**, 7–18.
- Jayaraman, A., W. Klement, Jr. and G.C. Kennedy, 1963; Melting and polymorphism of barium at high pressures, *Phys. Rev. Letters*, **10**, 387–389.
- Jayaraman, A., R.C. Newton and J.M. McDonough, 1967; Phase relations, resistivity, and electronic structure of cesium at high pressures, *Phys. Rev.*, **159**, 527–533.
- Kennedy, G.C. and P.N. LaMori, 1962; The pressure of some solid-solid transitions, *J. Geophys. Res.*, **67**, 851–856.
- Klement, W., Jr., A. Jayaraman and G.C. Kennedy, 1963; Phase diagrams of arsenic, antimony and bismuth at pressures up to 70 kbars, *Phys. Rev.*, **131**, 632–637.
- Lloyd, E.C., ed., 1971; *Symposium on Accurate Characterisation of High Pressure Environment*, 1968, N.B.S. Spec. Publ. 326, N.B.S., Washington, 333 pp.
- Matsushima, S., 1972; Compressional wave velocity in olivine nodules at high pressure and temperature, *J. Phys. Earth*, **20**, 187–195.
- Shimada, M., 1971; Measurement of pressure at high temperatures in a piston-cylinder apparatus, *Contr. Geophys. Inst. Kyoto Univ.*, **11**, 213–229.
- Shimada, M., 1972; Melting of albite at high pressures under hydrous conditions, *J. Phys. Earth*, **20**, 59–70.
- Shimada, M., 1974; On the quartz-coesite transition—Effect of the pressure medium on the generated pressure in a piston-cylinder apparatus—, read at the Meeting, Seism. Soc. Japan, Shimizu, May 11, 1974.
- Watanabe, H., 1972; Measurements of electrical conductivity of granite under high pressures, *Contr. Geophys. Inst. Kyoto Univ.*, **12**, 177–186.
- Wilson, W.B., 1960; Device for ultra-high-pressure high-temperature research, *Rev. Sci. Instr.*, **31**, 331–333.
- Young, A.P., P.B. Robbins and C.M. Schwartz, 1963; Description and calibration of a modified girdle high-pressure high-temperature apparatus, in *High-Pressure Measurement*, edited by A.A. Giardini and E.C. Lloyd, Butterworths, Washington, 262–273.
- Yukutake, H., 1974; Anisotropic thermal diffusivity of quartz at high pressures and temperatures, *J. Phys. Earth*, **22**, in press.